Decentralized stabilization of large-scale civil structures

Lubomír Bakule, Martin Papík and Branislav Rehák

Institute of Information Theory and Automation
Academy of Sciences of the Czech Republic
182 08 Prague 8, Czech Republic (bakule,papik,rehakb@utia.cas.cz)

Abstract: The objective of this investigation is to present a decentralized design of decentralized controllers for a 20-story steel structure benchmark. The benchmark problem was proposed within the structural control community to design and compare control schemes for seismically excited buildings. The control design problem is focused on an in-plane analysis of one-half of the structure. The height of the building naturally suggests the disjoint decomposition of a finite element overall dynamic model into two subsystems, each covering 10 stories. Inter-story elements appearing between the 10th and the 11th fool serve as the coupling elements of the overall interconnected system. The idea of decentralization of control has been numerically tested and compared to the benchmark sample centralized LQG design. The performance of the decentralized control design has been assessed by means of given benchmark evaluation criteria, eigenvalue analysis and time responses for both pre-earthquake and post-earthquake structures.

Keywords: Decentralized control, efficient strategies for large scale complex systems, monitoring and control of spatially distributed systems

1. INTRODUCTION

Large-scale complex systems refer generally to the large size and complexity of systems when considering the formulation of control laws. Particularly, large size, uncertainty, information structure constraints, and delays are standardly the motivating issues for development of decentralized control strategies including the concurrent development of numerically efficient computational algorithms. It is usually convenient to represent large-scale system as a collection of coupled subsystems. It generates a subsequent need to develop efficient decomposition algorithms that are based exclusively on the structure of a given system.

1.1 Prior Work

Large-scale system control problems and the methodologies to overcome particular complexity problems generated by these systems have been are are being developed since the 1970s. The relevant methodologies are surveyed in detail for instance in Bakule and Lunze [1988], Šiljak [1991], Bakule [2008], Zečević and Šiljak [2010].

Large flexible structures are just one of many practical applications where decentralized control strategies have been and are currently being applied. It is well known that the control of flexible structures represents a new, difficult and unique problem, with many complexities in the processes of modelling, control design and implementation. Benchmark structural models have been proposed in recent years as challenging problems to the structural control community to design and compare control schemes for flexible structures subjected to vibration excitations Housner et al. [1997], Spencer Jr. et al. [1998], Dyke et al. [2003], Gawronski [2004], Bakule et al. [2005], Preumont [2011]. Decentralized control strategies for building structures have been studied within lumped models in Lei et al. [2012], Lei and Wu [2011], Lei et al. [2013], Li et al. [2011], Seth et al. [2005], Wang et al. [2005].

The paper attempts to explore the possibility of decentralized design of decentralized controllers by using disjoint decompositions for the 20-story building benchmark control problem proposed in Spencer Jr. et al. [1998]. The problem is based on the decomposition of a 20-story steel building structure into two disjoint substructures followed by the LQG design. The building is described by a high-fidelity linear time-invariant state space model and designed as the true evaluation model. Sixteen evaluation criteria measuring the effectiveness of proposed control strategies are given. They quantify the reduction of undesired responses of the evaluation mode to ground excitation along with the associated design constraints such as energy consumption. Four different records of real-world earthquakes are used for each simulation run. Two different models are used for each run, i.e. pre-earthquake and post-earthquake structures which differ in the values of the system parameters. The benchmark problem includes the results of the sample example which is based on the centralized control LQG design. This case has been selected as a reference case for the comparison of the results.

To the authors best knowledge, the problem of decentralized LQG design for in-plane (2D) 20-story benchmark building problem has not been solved up to now.

1.2 Outline of the paper

In this study, the simplest case of decentralized design of decentralized controllers is considered for the overall finite element on in-line (2D) pre- and post-earthquake models (FEM) to illustrate the potential of this approach. Particularly, each overall model is considered as composed of two disjoint subsystems with disjoint coupling. The first subsystems is composed of the building structure of the 1-10th floors, while the second subsystem is composed of the remaining structure between the 11-20th floors. The couplings are the parts of the columns between the 10th and the 11th floors. Identical models and location of all sensors is used as those ones in the sample centralized case. A total of 56 actuators have been selected with their particular locations on the floors. The main reason for this selection is that, in order to conclude on the potential benefits of an decentralized control scheme, it is a standard step to compare the performance with the one of a centralized control scheme. The design procedure is based on the decomposition of the overall systems into two subsystems by neglecting the coupling terms. Then, the necessary model reductions for each subsystem are performed. Subsequently, the local LQG design with an infinite time horizon is adopted for each reduced subsystem of the post-earthquake model. Finally, the local LQG controllers are implemented into the original overall system. And, the performance, calculation of evaluation criteria given in the benchmark problem, and analysis of time history response for selected earthquake excitations are applied on both pre- and post-earthquake models.

2. PROBLEM STATEMENT

Consider the 20-story building structure illustrated in Figure 1. A complete physical description of the 20-story building benchmark problem, i.e. a finite element model and a Matlab/Simulink simulation framework are given in Spencer Jr. et al. [1998]. Suppose the sensor and their locations are identical with those ones used in the sample control system design example.

The objectives of this study are the following:

(1) To propose a convenient decomposition of the building structure into disjoint subsystem/interconnection structure.
(2) To propose well operating number of actuators including their locations on the floors.
(3) To design a decentralized LQG active control strategy.
(4) To perform simulations to assess the dynamic behavior of the benchmark model when using the implemented decentralized control.
(5) To assess the performance of the decentralized control by calculating evaluation criteria, analyzing responses and eigenvalues under all benchmark earthquake excitations.

The input excitation of the building structure is supposed to be one of the four real world historical earthquake

records: (i) *El Centro* (1940), (ii) *Hachinohe* (1968), (iii) *Northridge* (1994), and (iv) *Kobe* (1995). The N-S component of each earthquake record is used as the model input. Each proposed control strategy is evaluated for all earthquake records.

3. SOLUTION

First, sensor and actuator models as well as their location must be defined. Suppose the sensor and their locations are identical with those ones used in the sample control system design example. They are located on floors 5,9,13,17, and the roof. The section is divided into three parts: Decomposition and actuators, Control design and Simulation results.
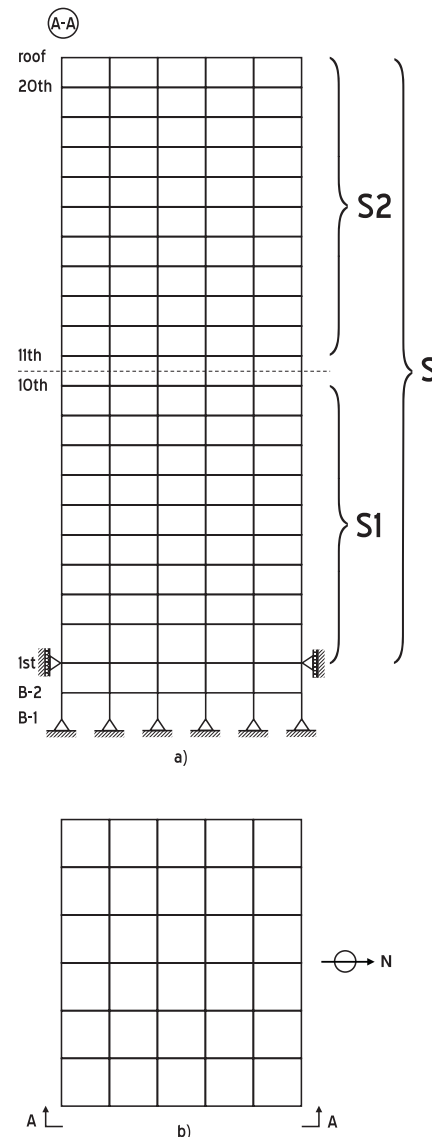

Fig.1. Building structure and its decomposition

Fig.1a shows the elevation of the structure. The levels are of the building are numbered with respect to the first story located at the ground level. The 21st level is denoted the roof and two basement level are denoted B1 and B2. The structure denoted as S is decomposed into two design

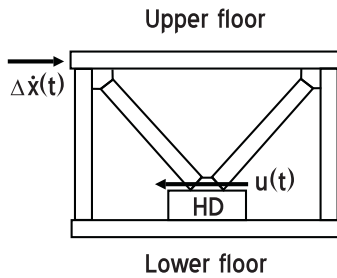model substructures $S1$ and $S2$. Fig.1b shows the plan of the structure.

Fig.2. Hydraulic damper located between two floors

3.1 Decomposition and Actuators

The decomposition of the original FEM model S into two subsystems $S1$ and $S2$ is proposed as shown in Fig.1. The system S has 540 DOFs prior the realization of the corresponding boundary conditions. The coupling terms between the 10th and the 11th floors include not only the parts of the steel columns of the building but also the control device located between these floors. The implementation of a hydraulic actuator is shown in Fig.2. In general, the actuators require the information from both the ith and the $(i + 1)$th floors. For instance the desired force $u(t)$ generated by the actuator HD is in an opposite direction to the inter-story velocity $\Delta \dot{x}(t)$. It means that the elimination of the disjoint coupling terms must include also the elimination of the corresponding control devices. The subsystems $S1$ and $S2$ have 2 and 3 measured outputs, and 9 and 10 control inputs, respectively.

Hydraulic actuators are located on each floor except the 10th floor. A total of 56 actuators are used. The numbers of actuators and their location on the floors are based on the analysis of physical properties of the decomposed structure. These numbers are from the bottom to the roof 2, 1, 1, 1, 1, 1, 1, 1, 7, 0, 4, 4, 4, 4, 4, 4, 4, 4, 4, 4.

More precisely, the original mass and stiffness matrices have the order of 540 with two block diagonal blocks of the order 270. These matrices are reduced to 526 DOFs by excluding the elements, which are firmly attached to the ground. The matrices describing a lower subsystem $S1$ are reduced to 256 DOFs. The matrices describing an upper subsystem $S2$ are not reduced, i.e. its dimension remains unchanged. Then, the Ritz and Guyan reduction follow. It results in a reduced mass and stiffness matrices of order 106 with a block diagonal structure, where the lower and the upper blocks have the dimensions 49 and 57. The corresponding state-space system has the dimension 212. The subsequent model reduction results in the systems $S1R$ and $S2R$ of the dimensions 26 and 24, respectively. It remains to add 19 equations of the actuators which are divided as 9 and 10 for the subsystems $S1R$ and $S2R$, respectively. Therefore, the closed-loop reduced-order control design system SRC has the dimension 69 with the local closed-loop subsystem dimensions of order 35 and 34.

The number, locations and models of sensors has been selected identically with the sample example by Spencer Jr. et al. [1998]. Such sensors distribution save the wired costs

without any information constraints due to the observer. The minimal number and the location of actuators results is selected to reach acceptable values of the evaluation criteria and the structure responses. Only one decomposition of the structure is applied to serve as a methodological prototype case. Other decompositions are omitted here due to the space limitation.

3.2 Control Design

A large size of the model of building structure requires the model reduction. First, the mass and stiffness matrices are reordered into active and dependent DOFs. The dependent DOFs are reduced out for both the systems $S1$ and $S2$. Then, the Guyan reduction is applied on both subsystems. Finally, the order of state-space models for both substructures is reduced preserving input-output relationships. The orders of the resulting reduced control design systems $S1R$ and $S2R$ corresponding with the subsystems $S1$ and $S2$ are 26 and 24, respectively. The LQG design is performed for the systems $S1R$ and $S2R$, the decentralized observer-controller with 19 control devices is implemented into the evaluation model of the order of 231. Then, the overall closed-loop system performance is evaluated on the evaluation model.
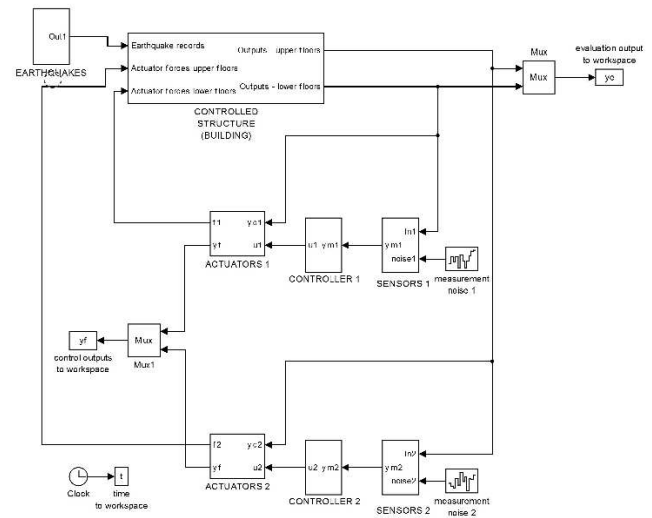

Fig.3. Simulink model of decentralized control design

The decomposition as well as the model reductions and the LQG control design are standard design procedures. Simulink scheme which is shown in Fig. 3 illustrates two local feedback loops with the controllers designed for the reduced subsystems $S1R$ and $S2R$.

Computational algorithm follows:

Algorithm.

(1) Decompose the FEM model S into into two subsystems $S1$ and $S2$ by cutting the connections between the 10th and the 11th floors.
(2) Perform the partitioning of the mass and stiffness matrices into active and dependent DOFs, condense out the dependent DOFs, and apply the Guyan reduction on the systems $S1$ and $S2$.

(3) Construct the state-space model for both post-earthquake subsystems models and apply the model reduction. Select a minimal order of the subsystem's states ensuring the stability of the reduced-order models.

(4) Perform the LQG design with preselected weighting matrices for reduced order subsystems.

(5) Implement the local controllers into the original overall FEM model and run simulations.

(6) Evaluate the results by computing the given benchmark evaluation criteria, the dynamic responses and eigenvalues for both pre-earthquake and post-earthquake evaluation models. If the evaluation results are satisfactory goto (7), else goto (4) and tune the control design with different weighting matrices.

(7) End.

Algorithm presents the steps of decentralized design of decentralized controllers. Decomposition at the level of the original FEM model is necessary because the subsequent model reduction requires the balance realization operating only with the subsystem's states. The model reduction and the LQG design are performed using well-known algorithms. Matlab/Simulink and Control System Toolbox are used to help in this design and also to perform the numerical evaluations. Fig. 3 shows the Simulink diagram with the two decentralized controllers. Local feedback loops use only local states. There are no actuators in the couplings.

The resulting controller gain matrix K has the dimensions 19x69. It is composed of the block matrices $K1$ and $K2$ of dimensions 9x35 and 10x34, respectively. The resulting observer gain matrix L has the dimensions 69x5. It is composed of the block matrices $L1$ and $L2$ of dimensions 35x2 and 34x3, respectively.

3.3 Simulation Results

A systematic evaluation of the performance is based on the evaluation criteria $J_1 - J_{16}$. The criteria $J_1 - J_{15}$ are those ones used by Spencer Jr. et al. [1998]. The criterion J_{16} has been added. It is the value of the maximal actuator force corresponding with the current simulation run. It is required to keep this value less than the capacity of 897 kN which is allowed for used hydraulic actuators. The criteria $J_1 - J_3$ have been selected as the most significant criteria. More precisely, these criteria are defined as follows

$$J_1 = \max_E \left(\frac{\max_{t,i} |x_i(t)|}{x^{max}} \right) \tag{1}$$

where J_1 denotes the maximum displacement over the set of all states $x_i(t)$ corresponding to the horizontal displacement of floors relative to the ground. x^{max} is the maximum uncontrolled displacement and over all four earthquakes denoted as E.

$$J_2 = \max_E \left(\frac{\max_{t,i} |d_i(t)|}{d^{max}} \right) \tag{2}$$

where J_2 denotes the maximum inter-story drift over the set of all states $x_i(t)$ corresponding to the drift of floors. d^{max} is the maximum inter-story drift and over all four earthquakes denoted as E.

$$J_3 = \max_E \left(\frac{\max_{t,i} |\ddot{x}_{ai}(t)|}{\ddot{x}_a^{max}} \right) \tag{3}$$

where J_3 denotes the maximum floor accelerations. corresponding to the drift of floors. $\ddot{x}_a^{max}$ is the maximum uncontrolled floor acceleration corresponding to each earthquake from E.

A short summary of the evaluation criteria follows:

J_1 -Floor displacement
J_2 -Inter-story drift
J_3 -Floor acceleration
J_4 -Base shear
J_5 -Normed floor displacement
J_6 -Normed inter-story drift
J_7 -Normed floor acceleration
J_8 -Normed base shear
J_9 -Control force
J_{10} -Control device stroke
J_{11} -Control power
J_{12} -Normed control power
J_{13} -Control devices
J_{14} -Sensors
J_{15} -Computational resources
J_{16} -Maximum actuator force

Note that the values of the criteria $J_1 - J_8$ are equal to one, while the values of the remaining criteria are equal to zero for the uncontrolled system. Any successful controller design corresponds with the values of criteria $J_1 - J_8$ less than one. The post-earthquake model has decreased stiffness caused by assumed structural damages compared with the pre-earthquake model. Simulations have shown that the usage of the post-earthquake model for the control design with a subsequent verification on the closed-loop system composed of the pre-earthquake model with the feedback gain matrices generated for the post-earthquake model is more convenient approach than the usage of these models in the opposite order. Therefore, the proper decentralized LQG design has been performed for the post-earthquake model as the case corresponding with the worst possible scenario.

	ElCentro	Hachinohe	Northridge	Kobe
J_1	0.8079	0.6593	0.7835	0.7213
J_2	0.8270	0.6956	0.8610	0.5960
J_3	0.9763	0.6546	0.7415	0.8040
J_4	0.8303	0.6666	0.9074	0.6240
J_5	0.6807	0.5663	0.5807	0.7069
J_6	0.6779	0.5759	0.5934	0.6710
J_7	0.5793	0.5380	0.5300	0.6367
J_8	0.6403	0.5341	0.5524	0.6728
J_9	0.0051	0.0052	0.0164	0.0150
J_1	0.0682	0.05358	0.0698	0.7342
J_{11}	0.0084	0.0064	0.0240	0.0175
J_{12}	0.0192	0.0186	0.0557	0.0630
J_{13}	56	56	56	56
J_{14}	5	5	5	5
J_{15}	69	69	69	69
J_{16}	235.2	280.9	890.1	692.5

Tab.1. Pre-earthquake performance

	ElCentro	Hachinohe	Northridge	Kobe
J_1	0.8932	0.9776	0.8010	0.7079
J_2	0.8286	0.9842	0.8442	0.6197
J_3	0.9991	0.9294	0.8370	0.9000
J_4	1.1190	1.0330	0.9919	0.7479
J_5	0.5967	0.5999	0.6385	0.5196
J_6	0.6106	0.6482	0.6256	0.5054
J_7	0.7372	0.6097	0.5195	0.6441
J_8	0.5746	0.5498	0.5356	0.5010
J_9	0.0040	0.0041	0.0139	0.0119
J_{10}	0.0797	0.0990	0.0944	0.0736
J_{11}	0.0049	0.0060	0.0198	0.0126
J_{12}	0.0173	0.0178	0.0523	0.0446
J_{13}	56	56	56	56
J_{14}	5	5	5	5
J_{15}	69	69	69	69
J_{16}	181.1	225.8	756.4	593.5

Tab.2. Post-earthquake performance

Direct comparison of the maximal values over all criteria and earthquakes surveys the following table

	pre-	post-
J_1	0.8079	0.9776
J_2	0.8610	0.9842
J_3	0.9764	0.9991
J_4	0.9074	1.1190
J_5	0.7069	0.6385
J_6	0.6779	0.6482
J_7	0.6367	0.7372
J_8	0.6728	0.5746
J_9	0.0164	0.0139
J_{10}	0.0734	0.0990
J_{11}	0.0240	0.0197
J_{12}	0.0630	0.0523
J_{13}	56	56
J_{14}	5	5
J_{15}	69	69
J_{16}	890.1	756.4

Tab.3. Maximal values of the criteria

It is observed from above tables that the values of the main criteria $J_1 - J_3$ are less than one and hydraulic actuators with a capacity of 897 kN do not exceed the maximum force capacity over all four earthquakes. Note only J_4 is little greater than one also in the sample example which is considered as acceptable. The centralized sample example values of the criteria $J_1 - J_{16}$ are completely available for comparison in Spencer Jr. et al. [1998].

The responses in Figs.4-7 have been selected as the worst possible cases of the displacement and the norm of the vector of drifts over all floors and earthquakes. The responses on the Northridge earthquake record has been selected as the most appropriate case. Decentralized (Bold solid), sample example (Thin solid) and uncontrolled system (Dotted) dynamic responses are supplied. The plots illustrate the effectiveness of the presented approach.

The responses are little worse when comparing them with the centralized sample example, but they much better than

those ones of the uncontrolled system. The decentralized setting offers the advantage of low dimensional gain matrices, parallel operation of local controllers and simplified analysis of controller failures.
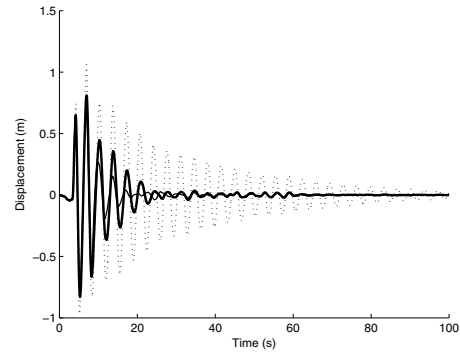

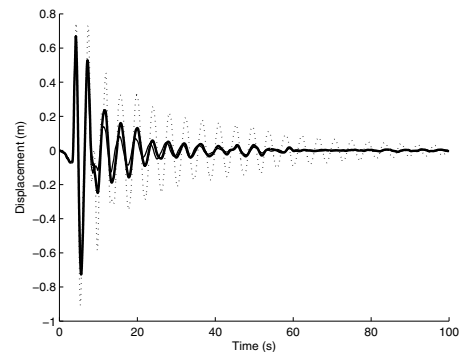Fig.4. Pre-earthquake: The 20th floor displacement

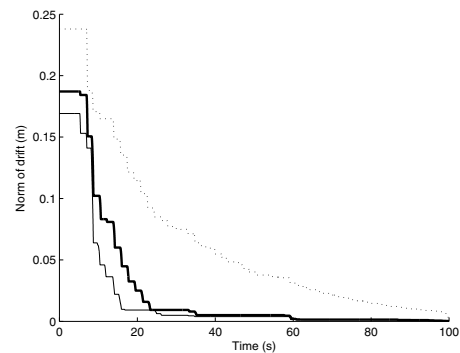Fig.5. Post-earthquake: The 20th floor Displacement

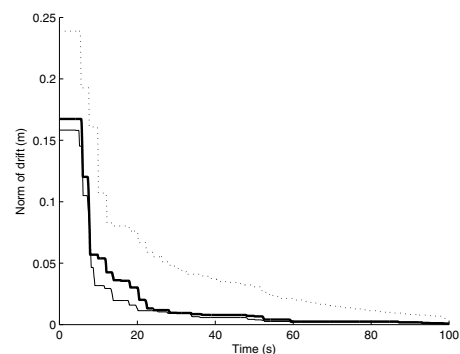Fig.6. Pre-earthquake: Norm of the vector of drifts

Fig.7. Post-earthquake: Norm of the vector of drifts

The last set of the results compares first ten natural frequencies of the designed closed-loop system (cont) with those ones of the uncontrolled system (uncont) and the sample example (sample) for both pre-earthquake and post-earthquake cases as follows

Pre-			Post-		
uncont	cont	sample	uncont	cont	sample
1.87	1.85	1.90	1.55	1.54	1.55
5.39	3.92	2.39	4.48	4.05	2.46
9.27	5.32	5.26	7.70	4.34	4.32
13.0	6.05	5.76	10.8	6.13	5.95
17.0	8.19	8.57	14.1	7.53	7.20
19.3	8.28	9.69	15.8	8.26	8.96
21.2	9.49	11.59	17.6	8.46	9.89
22.2	10.8	11.74	18.1	10.3	11.33
25.6	11.0	12.92	21.2	10.8	12.47
30.4	12.1	14.75	25.1	11.8	13.35

Tab.4. Natural frequencies comparison

The first mode is only little changed. The remaining modes are changed more. They are moved to lower frequencies. It may be interpreted as a better performance of the decentralized closed-loop system in comparison with the uncontrolled building structure, but worse when considering the sample example modes.

4. CONCLUSION

The paper presents simulation results of the decentralized design of decentralized LQG controllers for the 20-story 2D benchmark problem performed by using Matlab and Simulink. The main motivating ideas and objectives is the study of a potential usefulness of this approach for active control of large building structure. Decentralized control strategies offer generally the increase of operational reliability, reduction of communication costs and possibility of parallel implementation in real time when comparing them with centralized control issues. The building was decomposed into two disjoint subsystems, where the couplings are the parts of the columns between the 10th and the 11th floors. By properly identifying the nodes in the overall benchmark finite element model of the structure, it is possible to specify state space models for each subsystem. The benchmark sample centralized LQG design was selected as a reference for decentralized control design. The decentralized model has used the same models and locations of sensors but a little higher number and different locations of actuators as in the sample example case. The model reductions has been applied on each subsystem. The reduced order post-earthquake subsystems are used as the models for the LQG design. The evaluation has been performed on the original FEM model with the implemented local controller for both pre- and post-earthquake models. The performance assessment based on the benchmark evaluation criteria, the analysis of selected responses and the eigenvalues have been adopted for all prototype earthquakes.

The results look promising and confirm expectations. They are slightly worse than in the case of sample centralized case but lie within acceptable ranges. This encourages applying various system decomposition strategies as well as wired and wireless decentralized control design methodologies to the civil structure benchmark problem in the future.

REFERENCES

L. Bakule. Decentralized control: An overview. *Annual Reviews in Control*, 32:87–98, 2008.

L. Bakule and J. Lunze. Decentralized design of feedback control for large-scale systems. *Kybernetika*, 24(3–6): 1–100, 1988.

L. Bakule, F. Paulet-Crainiceanu, J. Rodellar, and J.M. Rossell. Overlapping reliable control for a cable-stayed bridge benchmark. *IEEE Transactions on Control Systems Technology*, 13(4):663–669, 2005.

S.J. Dyke, J.M. Caicedo, G. Turan, L.A. Bergman, and S. Hague. Phase I benchmark control problem for seismic response of cable-stayed bridges. *ASCE Journal of Structural Engineering*, 129(7):857–872, 2003.

W.K. Gawronski. *Advanced Structural Dynamics and Active Control of Structures*. Springer, New York, 2004.

G. W. Housner, L. A. Bergman, T. K. Caughey, A. G. Chassiakos, R. O. Claus, S. F. Masri, R. E. Skelton, T. T. Soong, B. F. Spencer, and J. T. P. Yao. Structural control: past, present, and future. *Journal of Engineering Mechanics ASCE*, 123 (9):897–971, 1997.

Y. Lei and D.T. Wu. A new decentralized control approach for the benchmark problem. *Procedia Engineering*, 14: 1229–1236, 2011.

Y. Lei, D.T. Wu, and Y. Lin. A decentralized control algorithm for large-scale building structures. *Computer-Aided Civil and Infrastructure Engineering*, 27:2–13, 2012.

Y. Lei, D.T. Wu, and S.-Z. Lin. Integration of decentralized structural control and the identification of unknown inputs for tall shear bulding models under unknown earthquake excitation. *Engineering Structures*, 52:306–316, 2013.

H. Li, J. Wang, G. Song, and L.Y. Li. An input-to-state stabilizing control approach for non-linear structures under strong ground motions. *Structural Control and Health Monitoring*, 18(2):227–240, 2011.

A. Preumont. *Vibration Control of Active Structures. An Introduction*. Springer Verlag, Berlin Heidelberg, 2011.

S. Seth, J.P. Lynch, and D.M. Tilbury. Wirelessly networked distributed controllers for real-time control of civil structures. In *Proceedings of the American Control Conference*, pages 2946–2952, Portland, OR, 2005.

B.F. Spencer Jr., R. Christenson, and S.J. Dyke. Next generation benchmark control problem for seismically excited buildings. In *Proceedings of the Second World Conference on Structural Control, (sstl. cee.illinois.edu.benchmarks/bench2def/ngbench.pdf)*, pages 1351–1360, Kyoto, Japan, 1998.

D.D. Šiljak. *Decentralized Control of Complex Systems*. Academic Press, New York, 1991.

Y. Wang, K.H. Law, and S. Lall. Time-delayed decentralized H_∞ controller design for civil structures: a homotopy methor through linear matrix inequalities. In *Proceedings of the American Control Conference*, pages 4549–4556, Portland, OR, USA, 2005.

A. Zečević and D.D. Šiljak. *Control of Complex Systems. Structural Constraints and Uncertainty*. Springer Verlag, Berlin–Heidelberg, 2010.